The Solution Structure of the Four-Way DNA Junction at Low-Salt Conditions: A Fluorescence Resonance Energy Transfer Analysis

Robert M. Clegg,* Alastair I. H. Murchie,‡ and David M. J. Lilley‡
*Department of Molecular Biology, Max Planck Institute for Biophysical Chemistry, Göttingen, Germany, and ‡CRC Nucleic Acid Structure Group, Department of Biochemistry, The University, Dundee, Scotland

ABSTRACT The four-way DNA (Holliday) junction is an important postulated intermediate in the process of genetic recombination. Earlier studies have suggested that the junction exists in two alternative conformations, depending upon the salt concentration present. At high salt concentrations the junction folds into a stacked X structure, while at low salt concentrations the data indicate an extended unstacked conformation. The stereochemical conformation of the four-way DNA junction at low salt (low alkali ion concentration and no alkaline earth ions) was established by comparing the efficiency of fluorescence resonance energy transfer (FRET) between donor and acceptor molecules attached pairwise in three permutations to the 5′ termini of the duplex arms. A new variation of FRET was implemented based upon a systematic variation of the fraction of donor labeled single strands. The FRET results indicate that the structure of the four-way DNA junction at low salt exists as an unstacked, extended, square arrangement of the four duplex arms. The donor titration measurements made in the presence of magnesium ions clearly show the folding of the junction into the X stacked structure. In addition, the FRET efficiency can be measured. The fluorescence anisotropy of the acceptor in the presence of Mg^{2+} during donor titrations was also measured; the FRET efficiency can be calculated from the anisotropy data and the results are consistent with the folded, stacked X structure.

INTRODUCTION

The four-way junction structure is postulated to be important as an intermediate in recombination events (Holliday, 1964; Meselson and Radding, 1975; Orr-Weaver et al., 1981), particularly for the integrase class of site-specific recombination (Kitts and Nash, 1987; Nunes-Düby et al., 1987; Hoess et al., 1987; Jayaram et al., 1988). We have proposed a working model for the high salt structure of the folded four-way DNA junction, termed the stacked X-structure, based upon experimental and stereochemical considerations (Duckett et al., 1988; Murchie et al., 1989; von Kitzing et al., 1990; Clegg et al., 1992). In the presence of sufficient cations, the junction undergoes pairwise stacking of helical arms, to generate two quasicontinuous, coaxial helices (Fig. 1 *a*) that are rotated in the form of a right-handed X shape. The exchanging strands are disposed across the small angle of the X, giving an approximately antiparallel alignment of the continuous strands. The antiparallel X structure is consistent with the results of gel electrophoresis (Gough and Lilley, 1985; Cooper and Hagerman, 1987; Duckett et al., 1988), fluorescence resonance energy transfer (FRET) experiments (Murchie et al., 1989; Clegg et al., 1992), electric birefringence measurements (Cooper and Hagerman, 1989), and magnetic birefringence and neutron scattering experiments (Torbet et al., unpublished observations). The twofold symmetry of the structure is in agreement with experiments in which junctions were probed with hydroxyl radicals (Churchill et al., 1988). The folded structure of the four-way junction involves close juxtaposition of the folded structure of the DNA helices, and there is an optimal stereochemical arrangement in the right-handed, antiparallel structure whereby the continuous strands are accommodated in the major grooves of the opposed helices (Murchie et al., 1989; von Kitzing et al., 1990). The interaction of counter-ions is probably required to reduce the mutual repulsions of the negative charges in the region of the exchanging strands.

In the absence of added metal ions the four-way junction appears to have a conformation that is different from the folded stacked X structure. The molecular conformation in these very low salt conditions is not as well understood as the folded structure at higher ion concentrations. We observed marked differences in the gel electrophoretic migration of junctions, obtaining results consistent with a square configuration of arms (Duckett et al., 1988, 1990). The extended structure suggested was consistent with the reactivity of thymine bases at the point of strand exchange at low salt concentration, and we have observed chemical reactivity of bases at the junction of cruciform structures in supercoiled DNA at low salt concentrations (McClellan and Lilley, 1987). Our earlier FRET measurements (Clegg et al., 1992) showed low FRET efficiencies for all helical end-to-end vectors in solutions with low ion concentrations, indicating an extended structure under these conditions, but these data did not permit us to distinguish between possible structures (such as tetrahedral or square planar) with confidence. We therefore have extended these measurements and employed the donor titration experiment described in this paper to differentiate between possible low salt structures for the same junction (junction 3) that we have used to study the folded X structure in the presence of higher salt concentrations (Clegg et al., 1992). From these experiments we conclude

Received for publication 26 May 1993 and in final form 4 October 1993.
Address reprint requests to Dr. Robert M. Clegg, Max Planck Institute for Biophysical Chemistry, P. O. Box 2841, D-37018 Göttingen, Germany.

0006-3495/94/01/99/11 $2.00

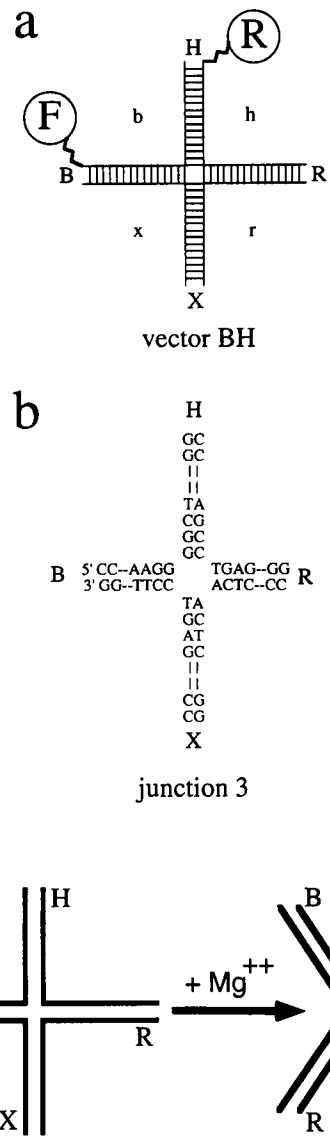

FIGURE 1 Construction of junction 3 and its study by fluorescence resonance energy transfer. (*a*) The junction is constructed by hybridization of four 34-base oligonucleotides (designated *b, h, r,* and *x*), to generate a structure comprising four 17-bp arms (designated *B, H, R,* and *X*). Two of the strands (*b* and *h* in the example illustrated) are conjugated at their 5′ termini with fluorophores, either fluorescein (*F*) or rhodamine (*R*). By these means the fluorophores are attached to the ends of selected arms (*B* and *H* in the example shown), and this can be repeated for other pairs of ends. In the donor titration experiment, the molar ratio of fluorescein conjugated/unconjugated strand (*b* as illustrated) is varied, while that of the acceptor is maintained at 1.0. (*b*) The sequence of junction 3 (Duckett et al., 1988; Clegg et al., 1992) used in these experiments. The central sequence around the point of strand exchange is shown, as well as the 5′CC termini present on each arm. (*c*) The ion-dependent folding of the junction. In the presence of added cations the junction is folded into the stacked X-structure (*right*). However, in the absence of added ions the junction is unable to fold and remains in an extended, unstacked conformation (*left*).

that in the absence of added metal ions the junction adopts a configuration in which the arms are directed toward the corners of a square.

Fluorescence resonance energy transfer (FRET) is becoming a powerful method for the study of the conformation of folded nucleic acid structure in solution (Murchie et al., 1989; Clegg et al., 1992; Clegg, 1992; Cardullo et al., 1988; Jovin, 1991; Rippe et al., 1993). The conjugation of fluorescent dyes to well-defined synthetic single-stranded DNA is straightforward, and the separation of labeled oligomers from unlabeled (but otherwise identical) molecules can be carried out to yield very pure labeled single-strand (SS) molecules. We have recently used FRET to investigate the helical structure of DNA oligomers of varying length in solution and to measure the thermodynamic stability of these nucleic acid molecules (Clegg et al., 1993). This study also shows the reliability and robustness of the data analysis used in the present paper. By hybridization of complementary SS molecules that are 100% labeled with either donor *D* or acceptor *A* molecules, we can be confident that all multistranded molecules are labeled with both *D* and *A*. This is convenient because the extent of energy transfer depends not only on the distance and orientation between the *D* and *A* molecules but is also a strong function of the relative extent of labeling of the *D* and *A*. If a comparison between several related labeled macromolecules is to be made, or if quantitative estimates of the efficiency of FRET (*E*) is required, the average number of each dye molecule attached to the macromolecule must be known.

The extent of dye labeling is not usually employed directly as an experimental variable, although it is information crucial to the quantitive interpretation of the FRET results. The multistranded structures of nucleic acids permit quantitative manipulation of conjugated dye stoichiometry. This possibility is unique to macromolecules that associate by complementarity. A series of labeled DNA duplexes each with a different fraction of labeling with one chromophore constitutes a labeling "titration" series; other than the percentage labeling the DNA molecules are identical. A comparison of the predicted titration results with the actual series of FRET donor titration experiments provides a straightforward model for testing the reliability and precision of the FRET measurements. This serves as an additional criterion, indicating the reliability of the FRET measurements and data analysis by checking the agreement between a well-defined prediction and a simple experimental procedure. The donor titration method is applied here in conjunction with FRET to assist in two measurements: (*a*) to determine the symmetry of the four-way junction at low salt conditions by measuring the enhancement of the acceptor fluorescence, and (*b*) to determine the symmetry of the four-way junction at higher salt concentrations by measuring the fluorescence anisotropy. The results indicate an extended square structure at low salt, and the anisotropy FRET measurements at higher salt conditions are compatible with the folded X structure.

MATERIALS AND METHODS

Oligonucleotide synthesis

Oligonucleotides were synthesized using β-cyanoethylphosphoramidite chemistry (Beaucage and Caruthers, 1981; Sinha et al., 1984) implemented on a 394 DNA synthesizer (Applied Biosystems). 5′-amino groups at the

end of six-carbon linkers were introduced by means of a final coupling step with *N*-methoxytrityl-2-aminohexyl-2-cyanoethyl-*N,N*-diisopropyl amino phosphite (Connolly, 1987). Fully deprotected oligonucleotides were desalted and purified by anion exchange and reverse-phase HPLC. Pure oligonucleotides eluted as sharp peaks.

Conjugation with fluorescent dyes

Pure oligonucleotides were reacted with the *N*-hydroxy-succinamide ester of tetramethylrhodamine or fluoresceinisothiocyanate (Molecular Probes) (Murchie et al., 1989; Clegg et al., 1992), and unreacted dyes were removed by gel filtration on Sephadex G25 (Pharmacia). Dye-conjugated oligonucleotides were separated from unreacted DNA by electrophoresis in 20% polyacrylamide in 90 mM Tris borate (pH 8.3) and 7 M urea. Each conjugated oligonucleotide migrated as a single fluorescent band; the bands were excised, and the DNA was recovered by electroelution. Dye-conjugated DNA and unreacted oligonucleotides were separated by more than the equivalent electrophoretic mobility of one nucleotide. This method was designed to yield 100% labeled DNA, and this was confirmed spectroscopically.

Construction of junctions

Appropriate combinations of the dye-labeled and unconjugated oligonucleotides were hybridized in 450 mM NaCl, 24 mM Na citrate (pH 7.0), 2 mM $MgCl_2$ by slow cooling from 65 to 10°C. Junctions were assembled containing two unlabeled strands, one strand 100% labeled with rhodamine, and one strand as a mixture of unlabeled and fluorescein-conjugated DNA in selected proportion (molar ratios of fluorescein/rhodamine of 0.25, 0.5, 0.75, and 1.0). Junctions were purified by electrophoresis in 8% polyacrylamide gels in 90 mM Tris-borate (pH 8.3) and 2 mM $MgCl_2$ with circulation of the buffer. Bands containing four-way junctions were excised, and DNA was recovered by electroelution.

Preparation of junctions for spectroscopy

All labeled junction samples were precipitated from ethanol, dried under vacuum, and dissolved into the fluorescence buffer (90 mM Tris-borate, pH 8.3). Absorption measurements were made on these solutions (230–600 nm); these spectra were used to determine the concentration of the junctions (DNA and the probes), and in conjunction with the fluorescence measurements determined the consistency of the labeling efficiency (Fig. 2). All samples were measured at 20°C. For the series of junction measurements on junction 3, the salt was added from a concentrated Mg^{2+} solution in one step. The extent of labeling was verified by absorption measurements at 260, 496, and 558 nm. Absorption spectra of the dye molecules is not generally as sensitive to the conjugation or the molecular environment as fluorescence spectra.

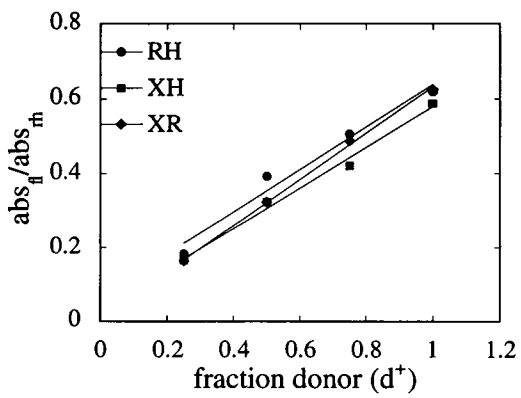

FIGURE 2 Plot of the ratio of fluorophore absorbances (abs_{fl}/abs_{rh}) versus d^+ for the three representative end-to-end vectors of junction 3. The end-to-end vectors RH, XH, and XR were prepared with 100% rhodamine (*rh*) labeling, and 25, 50, 75, or 100% fluorescein (*fl*) labeling.

Instrumentation

Absorption measurements were taken on either a Uvicon 820 (Kontron) or a Cecil CE6600 spectrophotometer. All steady-state fluorescence experiments were made with a SLM 8000S (Urbana, IL) instrument. Excitation and emission spectra were corrected for lamp fluctuations and instrumentation variations. Polarization artifacts were avoided by employing "magic angle" conditions (e.g., the angle of the linear polarizer relative to the vertical position is 54.5° for excitation and 0° for emission). Excitation and emission fluorescence spectra were acquired and processed with an LSI DEC computer. Each spectrum was fitted to a series of Chebyshev polynomials (De Boeck et al., 1985) to filter random noise. All energy transfer measurements were corrected for the contribution of the buffer. The standard fluorescence spectra for FRET were collected over a broad range of excitation and emission wavelengths (excitation spectra: λ_{ex} = 400–590 nm, λ_{em} = 600 nm; emission spectra: λ_{ex} = 490 nm, λ_{em} = 500–650 nm). The absorption of all solutions used for the fluorescence measurements at the wavelength of excitation was always below 0.015. Junctions that were singly labeled with fluorescein and rhodamine were also synthesized; the fluorescence spectra of these probes were used to decompose the doubly labeled fluorescence spectra into donor and acceptor components, as described below.

For the steady-state fluorescence anisotropy measurements the excitation and emission wavelengths were constant. The wavelengths (in nm) for excitation and emission for the anisotropy of fluorescein alone, for rhodamine alone, or for both donor and acceptor with FRET were, respectively, 490 and 520, 565 and 600, or 490 and 600.

DATA ANALYSIS FOR FRET DONOR TITRATION AND ANISOTROPY

Efficiency of energy transfer

The rate of nonradiative dipole-dipole energy transfer, k_T, from the singlet state of a donor D to the singlet state of an acceptor A is (Förster, 1949),

$$k_T = \left(\frac{R_0}{R}\right)^6 \Big/ \tau_D \qquad (1)$$

where $R_0 = 8.785 \times 10^{-23} \cdot \Phi_D \cdot \kappa^2 \cdot n^{-4} \cdot J(\nu)$ cm^6; Φ_D and τ_D are the emission quantum yield and lifetime of D in the absence of A; $J(\nu)$ is the overlap integral; R is the scalar D-A separation; n is the index of refraction of the condensed matter between D and A; and κ is the orientation factor for dipole-dipole coupling. R_0 for the fluorescein and rhodamine D-A pair is generally considered to be between 40 and 55 Å, although the value for each particular case of conjugated dyes can vary considerably due to the sequence of the DNA at the ends, length of the linker, and the solution conditions.

For a particular configuration of the donor and acceptor the efficiency of energy transfer E is defined in terms of kinetic constants of decay from the excited state of the donor, or in terms of R and R_0 by Eq. 1,

$$E = \frac{k_T}{\tau_D^{-1} + k_T} = \frac{1}{1 + (R/R_0)^6}. \qquad (2)$$

There may be several different configurations of D and A, each with possibly different values of R and R_0, in which case the observed efficiency is the appropriate average over the molecular ensemble.

We assume that κ^2 and R_0 have the same values for all the fluorescently labeled junctions. Sufficient rotational freedom of just the donor can render κ^2constant (Stryer, 1968); the value of $r_{\text{fluorescein}}$ (the fluorescence anisotropy of the fluorescein) is low enough that we can make a reasonable approximation that κ^2 is constant for all samples.

FRET donor titration analysis

Our previous measurements have shown that E is very small for FRET measurements at low salt with the four-way junctions described here. The expected efficiency of FRET is only a few percent.

The efficiency of energy transfer is measured from the induced emission of the acceptor as follows:

1. The fluorescein contribution from each energy transfer emission spectrum is removed by fitting the 500–530-nm portion (only fluorescein emits here) to a standard singly labeled fluorescein junction spectrum and subtracting this fluorescein emission component from the emission spectrum from 500 to 650 nm. Alternatively, a linear combination of standard donor and acceptor emission spectra (using singly labeled molecules) is fit to the entire emission spectrum, and the rhodamine fraction is then determined directly.
2. The resulting spectrum, consisting of only the rhodamine emission, is normalized by the maximum (or the integrated intensity between 530 and 570 nm) of the excitation spectrum from the same sample (an emission spectrum excited at ~565 nm can also be used for this purpose). The precision of the measurement is determined by measuring the repeatability of the quantities discussed below several times on certain junction vectors.

Normalizing the fluorescence emission to the concentration of molecules (step 2 above) is necessary for all FRET determinations, and achieving this with fluorescence spectral measurements on the samples alone has advantages (Conrad and Brand, 1968). The following is a quantitative description of the formalism just described and the explicit effect of the fraction of donor and acceptor labeling on the FRET analysis.

By using known fractions of unlabeled and labeled donor single strands of DNA with 100% labeled acceptor single strands, and separating specifically the double-stranded products, we can easily vary the fraction of donor labeling of the final structure. We define d^+ to be the fraction of the particular single-stranded oligomer that is actually labeled with D. d^- is the fraction of this oligomer that is unlabeled ($d^+ + d^- = 1$). a^+ and a^- refer to the same values for A.

The total emission measured from a solution of donor and acceptor labeled junctions, excited at frequency ν' and measured at ν, is

$$\begin{aligned} F(\nu, \nu') &\propto [S] \cdot [\epsilon^D(\nu') \cdot \Phi^A(\nu) \cdot E \cdot d^+ \cdot a^+ + \epsilon^A(\nu') \cdot \Phi^A(\nu) \cdot a^+ \\ &\quad + \epsilon^D(\nu') \cdot \Phi^D(\nu) \cdot d^+ \cdot \{(1 - E) \cdot a^+ + a^-\}] \\ &= F^A(\nu, \nu') + F^D(\nu, \nu'). \end{aligned} \tag{3}$$

The superscripts D and A refer to the donor and acceptor, $[S]$ is the concentration of the completely reassembled junction molecules, $\epsilon^D(\nu')$ is the molar absorption coefficient of the donor, $\Phi^D(\nu)$ is an emission spectrum shape function proportional to the fluorescence quantum yield of the donor, and $F^D(\nu,\nu')$ is the spectral component of the donor contributing to the total fluorescence emission spectrum. $\epsilon^A(\nu')$, $\Phi^A(\nu)$, and $F^A(\nu,\nu')$ are the corresponding parameters for the acceptor. $F^A(\nu,\nu')$ is derived from both direct excitation and energy transfer from the donor. The inclusion of the factors d^+, a^+, and a^- conveniently express the extents of labeling of the single-stranded moieties.

We define the term $F'(\nu, \nu')$ as the measured rhodamine component of the emission spectrum, after subtracting the fluorescein component; $F'(\nu, \nu')$ is composed of the first two terms in Eq. 3 (i.e., all terms having Φ^A). The measured spectrum $F'(\nu, \nu')$ corresponds to the theoretical expression $F^A(\nu, \nu')$ defined in Eq. 3.

$F'(\nu, \nu')$ is normalized by a fluorescence value of the rhodamine alone, measured in an excitation (or emission) spectrum as described above. To generalize, the measurement of rhodamine fluorescence alone with an excitation at ν'' is made with the emission at ν_2, and the FRET measurement with an excitation at ν' is made with an emission at ν_1. The following ratio is then formed:

$$\begin{aligned} (\text{ratio})_A &= \frac{F'(\nu_1, \nu')}{F(\nu_2, \nu'')} \\ &= \left\{ E \cdot d^+ \frac{\epsilon^D(\nu')}{\epsilon^A(\nu'')} + \frac{\epsilon^A(\nu')}{\epsilon^A(\nu'')} \right\} \cdot \frac{\Phi^A(\nu_1}{\Phi^A(\nu_2)}. \end{aligned} \tag{4}$$

$(\text{ratio})_A$ is linearly dependent on both d^+ and E. The $(\text{ratio})_A$ values reported here are calculated from an emission spectrum with $\nu' = 490$ nm and $\nu_1 \approx 585$ nm, and an excitation spectrum with $\nu'' \approx 560$ nm and $\nu_2 = 600$ nm; $\epsilon^A(\nu')/\epsilon^A(\nu'')$ and $\epsilon^D(\nu')/\epsilon^A(\nu'')$ are easily measured. If $\nu_1 = \nu_2$ the last term of Eq. 4 is 1. Of course, all instrumentation constants resulting from differences between the settings of the instrument for the excitation and emission spectra must be taken into account (this is not shown in Eq. 4). The correction factors can be calculated by comparing the last term of Eq. 4 with the intercept of the $(\text{ratio})_A$ versus d^+ plot of Fig. 3, or from measurements on singly labeled rhodamine junctions.

Measuring the normalized enhanced fluorescence of the acceptor according to Eq. 4 avoids certain experimental factors that could introduce uncertainty into the FRET measurement, and it is a robust and reliable measurement for our

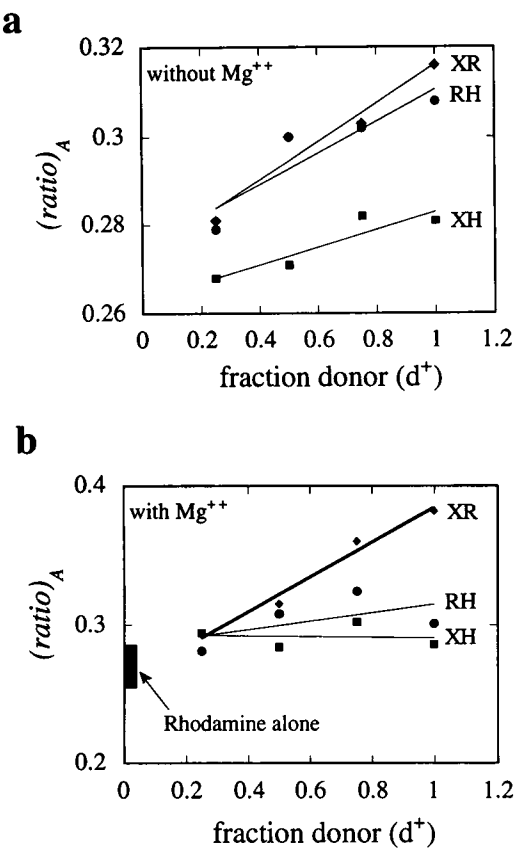

FIGURE 3 Enhancement of acceptor emission as a function of the fraction of donor labeling (d^+) for three representative end-to-end vectors of junction 3. The end-to-end vectors RH (●), XH (■), and XR (◆) were prepared with 100% rhodamine (*rh*) labeling and 25, 50, 75, or 100% fluorescein (*fl*) labeling. (*a*) Plot of $(\text{ratio})_A$ versus d^+ in the absence of added magnesium. (*b*) Plot of $(\text{ratio})_A$ versus d^+ in the presence of 5 mM $MgCl_2$.

situation. Some important points for our measurements are: (*a*) Φ^A does not enter directly into the $(\text{ratio})_A$, only the ratio $\Phi^A(\nu_1)/\Phi^A(\nu_2)$ at two wavelengths is needed; (*b*) a^+ does not enter into Eq. 4; (*c*) error in the percentage labeling of the donor (i.e., $\pm\Delta d^+$) will introduce this same percentage error into the derived value of E since the factor $E \cdot d^+$ enters directly into Eq. 4; (*d*) $\Phi^D(\nu_1)$, which can vary for different D environments, affects only the actual value of E, not the measurement directly.

Fluorescence anisotropy

Under certain circumstances, we can estimate the efficiency of FRET from the fluorescence anisotropy, and the donor titration series provides an opportunity to determine the reliability of such a measurement. The measured average anisotropy is the sum of the weighted anisotropies of each species. The weighting factors are the relative emission intensities at the excitation and emission wavelengths used for the anisotropy measurements. The anisotropy of directly excited rhodamine is fairly high (~0.24, at 20°C), and the contribution to the measured anisotropy from acceptor molecules that are excited by energy transfer is much lower (probably close to zero) because of the energy transfer process.Therefore, the measured anisotropy of fluorescence excited and collected where both D and A absorb and emit will decrease as the efficiency of FRET increases. The small increase in the donor anisotropy will not contribute significantly. For these measurements the anisotropy was measured by exciting at 490 nm and observing the emission at 590 nm, $r_{490,\,590}$. For the rest of this section, the first and second subscripts refer to the excitation and emission wavelengths in nanometers. The superscripts ex and em refer to excitation or emission fluorescence spectra, and superscripts D and A refer to the donor or the acceptor. For instance, $F^{\text{em}}_{490,\,590}$ is the fluorescence intensity of an emission spectrum excited at 490 nm and observed at 590 nm; and $F^{\text{em},\,D}$ is a fluorescence intensity from an emission spectrum of the donor alone, normalized to 1 at the maximum, observed at 590 nm, and excited at *any* wavelength (this assumes the shape of the spectrum is independent of the excitation wavelength); and $F^{\text{em},D}_{490,590}$ is the donor component of an emission spectrum excited at 490 nm and observed at 590 nm. The following expressions can be written:

$$F^{\text{em, D}}_{490,590} = \frac{F^{\text{em, D}}(590)}{F^{\text{em, D}}(518)} \cdot F^{\text{em}}_{490,518},$$

$$F^{\text{em, A}}_{490,590} = F^{\text{ex}}_{558,590} \cdot \frac{F^{\text{ex, A}}(490)}{F^{\text{ex, A}}(558)} \cdot [\text{correction factor for emission spectra}] \tag{5}$$

In our case,

$$\frac{F^{\text{ex, A}}(490)}{F^{\text{ex, A}}(558)} = \frac{\epsilon^{\text{ex, A}}(490)}{\epsilon^{\text{ex, A}}(558)},$$

where ϵ is a molar extinction coefficient. $F^{\text{em}}_{490,518}$ and $F^{\text{ex}}_{558,590}$ are the fluorescence of the donor (decreased by FRET) and the acceptor (with no enhancement from FRET) of a doubly labeled molecule without the interference from the complement of the D-A pair. The anisotropy r that is measured is

$$r_{490,590} = \frac{(F^{\text{em},D}_{490,590} \cdot r_D + F^{\text{em},A}_{490,590} \cdot r_A)}{F^{\text{em},D}_{490,590} + F^{\text{em},A}_{490,590} + F^{\text{em},A}_{490,590,\text{FRET}}}, \tag{6}$$

where r_D and r_A are the anisotropies of the donor and acceptor fluorophores, which are spectroscopically isolated (from the $F^{\text{em}}_{490,518}$ and $F^{\text{ex}}_{558,590}$ spectra) but in the doubly labeled DNA molecules, and $F^{\text{em},A}_{490,590,\text{FRET}}$ is the fluorescence intensity from the acceptor molecules that are excited by the FRET mechanism. In Eq. 6 it is assumed that the anisotropy contribution from $F^{\text{em},A}_{490,590,\text{FRET}}$ is zero, due to the energy transfer from statically and dynamically randomized orientations of the donor molecules, and that the anisotropy of the fluorescein is constant for all of the molecules that are compared in a titration series. This latter condition is expected since all donor labeled molecules are identical in that they all also have an acceptor.

RESULTS

Characterization of fluorescently labeled junctions

Absorption and fluorescence spectra and fluorescence polarization measurements show that our junctions are suitable for energy transfer measurements (see Clegg et al., 1992, for details and for an example of similar fluorescence spectra on such probes). Fig. 2 shows the ratio of the fluorescein absorbance (λ = 496 nm) to the rhodamine absorbance (λ = 600 nm) for all three junction isomers, as a function of the percentage donor labeling (d^+). The plot shows that the ratio of fluorescein to rhodamine is indeed that expected from the sample preparation; the small scatter in the data shows the precision of the percentage donor labeling and the agreement among the three sets of samples.

The fluorescence anisotropy measurements indicate that the fluorescein is very mobile within the fluorescence lifetime of 3–4 ns (Clegg et al., 1992). The fluorescence anisotropy of each fluorescence probe can be measured independently, even in the doubly labeled junctions, by measuring the fluorescence at the appropriate wavelengths (see Materials and Methods). At 20°C rhodamine conjugated to the junctions has an anisotropy of 0.25, and the fluorescein anisotropy (singly labeled) is 0.07 at low salt concentrations and 0.11 at the higher salt concentrations; this indicates that the fluorescein undergoes considerably faster rotational diffusion within a greater angular displacement than rhodamine. Such rapid movements of dyes within their excited state lifetime and random static orientations of the dye transition moments simplify the interpretation of energy transfer measurements (Förster, 1951; Steinberg, 1968).

FRET donor titrations at low and high salt concentration

Energy transfer was measured for the junction 3 isomers HR, XH, and XR, each labeled with 100% acceptor and 25%, 50%, 75%, and 100% donor. These isomers were chosen to typify the three possible dispositions of the donor and acceptor fluorophores, namely across the acute angle, across the obtuse angle, or on opposite ends of a quasicontinuous helix, according to the working model of the stacked X structure.

Plots of the $(\text{ratio})_A$ as a function of the percent donor labeling are given in Fig. 3, *a* and *b*. In Fig. 3 *a* are the donor titration measurements in the absence of added magnesium. One vector (XH) exhibits a consistently lower energy transfer ratio than the other two (HR and XR). This would be expected for an extended square structure, where the XH vector constitutes the diagonal of the square, while the HR and XR distances are shorter because they constitute two sides of the sequence. The intercepts of the straight lines are those expected from the 0% labeled donor duplex.

Fig. 3 *b* shows the analogous data obtained with magnesium added to the solution of the labeled junctions. The results are clearly different from those in the absence of added ions; under these conditions the XR shows consistently and significantly more energy transfer for any given extent of donor labeling than either the HR or XR vectors. This is consistent with the antiparallel X structure in which the B and X arms are stacked, resulting in the vector XR crossing the acute angle of the stacked X structure.

Donor titration analysis of anisotropy

The measured fluorescence anisotropy (r) from a solution of doubly labeled molecules depends upon the efficiency of FRET (see the data analysis section). Such fluorescence anisotropy measurements on the HR, XR, and XH vectors are presented in Fig. 4. The best fit of E according to Eq. 6 to the XR data (expected to have the highest efficiency of transfer from the above measurements) is shown bracketed by plots generated presupposing either no FRET or twice the fitted extent of FRET. The presence of FRET is clearly discernible, and the efficiency agrees with that determined from the analysis according to Eq. 6. The extent of FRET, measured by anisotropy, of the junction molecule with *D-A* labels juxtaposed across the acute angles according to the proposed X model (XR) can be clearly distinguished from the other two labeled isomers (HX and RH), which have longer expected distances separating the *D-A* pair according to the X model (across the obtuse angle, and over the distance of a quasicontinuous helix with a length of two arms).

DISCUSSION

The donor titrations presented above provide a measure for judging the precision of our FRET measurements.

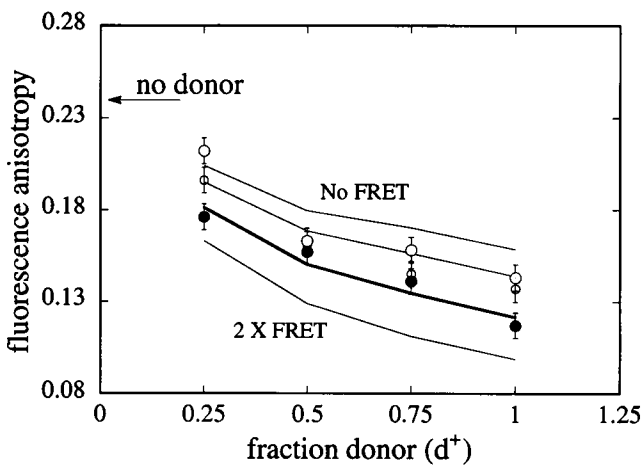

FIGURE 4 Plot of the fluorescence anisotropy $r_{490,590}$ (excitation at 490 nm and emission at 590 nm) for the end-to-end vectors RH, XH, and XR as a function of d^+. There are several ways to measure fluorescence anisotropy. The most common is: $r = (F_\parallel - F_\perp)/(F_\parallel + 2 \cdot F_\perp)$, where $F_\parallel$ = fluorescence signal measured with vertical excitation and emission polarizers, and $F_\perp$ = vertical excitation and horizontal emission polarizers, where the fluorescence is measured at right angles to the excitation beam. The lines are simulations according to Eq. 6 (see the text for an explanation of the terms in the equation); the bold line assumes E = 10%. The thin lines at the top and the thin line at the bottom are the simulations assuming no FRET and twice the amount of FRET indicated in the thick line. The middle thin line assumes E = 4%. The data are for the vectors: ○, XH; ○, RH; ●, XR. See the text for an explanation of the analysis.

Such titration experiments are naturally suited for nucleic acid samples with complementary sequences that form multiple-stranded nucleic acid structures. Similar titration experiments are often employed to titrate donor (acceptor)-labeled single strands into a solution of complementary acceptor (donor)-labeled single strands in order to determine the stoichiometric amounts of single strands needed to form duplexes (see, for instance, Cardullo et al., 1988); however, the goal and the experimental procedure of our present experiments are different. We have used the donor titrations to provide an additional experimental criterion to evaluate our determination of the relative extent of energy transfer of the differently labeled isomers of the four-way junction at low salt. The agreement of the donor titration results with the predictions of Eq. 4 supports our structural interpretation of the FRET results. The agreement between the intercept of Fig. 3 *a* and the measured $(\text{ratio})_A$ of double-stranded DNA junctions labeled only with the acceptor, and the expected linear plot of $(\text{ratio})_A$ versus d^+, shows that the incremental change in $(\text{ratio})_A$ as d^+ increases can be well determined. These two parameters (the intercept and the linearity of the plot) provide additional criteria for judging the precision of our FRET measurements.

As is evident from the data shown in this paper very small incremental values of E can be determined accurately by measuring the acceptor enhancement using the $(\text{ratio})_A$ analysis of the FRET data. The differentiation between small E values is comparatively difficult and less precise when observing the donor quantum yield alone (Clegg, 1992) (it involves determining small differences between large numbers). Determining E by measuring lifetimes of the donor fluorescence decay suffers from the same deficiency. For instance, it would be required to determine the fluorescence lifetimes of fluorescein (3–4 ns) within a precision of 30 to 100 ps in order to differentiate the different values of d^+ for one isomer or to distinguish between the labeled isomers.

Distinction between the FRET donor titrations using doubly labeled macromolecules and other related FRET experiments

The concentrations and ratios, $[D]/[A]$, of donor and acceptor molecules are often varied in FRET measurements, especially when the distances between the D and A molecules are not restrained by being attached to the same molecule. If the dye molecules are independently distributed in solution, the mean distance between D and A molecules will decrease as their concentrations increase, and this leads to a greater extent of energy transfer. The concomitant decreasing fluorescence intensity and polarization of the donor are the original observation that led to the development of the theory of fluorescence resonance energy transfer (Perrin, 1927; Förster, 1948). If the D and A molecules are distributed randomly in one, two, or three dimensions, and if FRET is operative the excited state of the donor does not decay exponentially (Förster, 1949); rather, the excited state of the donor decays as $e^{-(A \cdot t + B \cdot t^{D/6})}$, where the dimension of space is labeled by $D = 1$, 2, or 3 (see Hauser et al., 1976, and references therein). A and B are independent of time, and B is proportional to the concentration of A. For three dimensions the factor has been well documented (e.g., see Bennett, 1964; Mataga et al., 1969). If the density distribution follows a fractal power law, D is a noninteger; fractal analyses have been invoked to characterize polymer networks (Dewey, 1992; Drake et al., 1991). Key parameters in the above analyses are the distribution of A molecules surrounding the D molecules and the ratio $[D]/[A]$.

FRET can be useful for detecting the close association of two interacting (but translationally independent) molecules labeled with D and A chromophores, and this is another instance where the $[D]/[A]$ ratio is varied. For instance, normal titration experiments have been used to determine the distributions and numbers of receptor sites on cell surfaces (Dale et al., 1981; Szöllősi et al., 1984; Jovin and Arndt-Jovin, 1989; Kubitscheck et al., 1991). Such titration experiments employ D- and A-labeled molecules that are translationally independent of each other (before forming a complex), and the distribution of D-A radial distances changes dramatically during the course of the titrations; the change in the average D-A separation is a major experimental variable.

In our FRET donor titrations with doubly labeled DNA molecules, only isolated D-A pairs with identical FRET characteristics are present in the solution, together with intact DNA molecules labeled solely with A. The spectroscopic parameters defining the efficiency of energy transfer of these D-A pairs are independent of the fraction of donor present, in contrast to the applications discussed in the last paragraph. The measured emission characteristics of the donor are independent of the extent of donor labeling because every donor molecule is attached to a DNA molecule that has a complementary acceptor (all DNA molecules have acceptors). The relative acceptor emission (i.e., ratio A, which is our measured, or rather derived, FRET parameter) does depend on the extent of donor labeling, but in a predictable fashion, according to Eq. 4. Fig. 3 shows that we are able to measure the relative FRET efficiencies with the accuracy necessary to distinguish the differently labeled isomers of the junction molecules in low salt conditions. The FRET data, together with the electrophoresis results (Duckett et al., 1988), imply that the arms of the four-way junction at low salt are oriented relative to each other in a square arrangement.

Structure of the junction in low salt solutions

We have shown previously that the extent of energy transfer for all six end-to-end vectors of the doubly labeled junction 3 in the absence of added salt is small, which is consistent with an extended structure. These small values of transfer were also modulated in an interesting way; the end-to-end vectors BR and HX were both lower than the remaining four vectors, indicating that the diagonal end-to-end distances were longer under these conditions. However, this difference was small, and the donor titration experiments presented here provided us with additional evidence to test this interpreta-

tion. The slopes of the straight lines show differences in the extent of energy transfer for different end-to-end vectors in the absence of Mg^{2+} (Fig. 3 *a*). Two of the labeled isomers exhibit more energy transfer (i.e., shorter distances) than the other, and as before (Clegg et al., 1992), it was the diagonal vector that was associated with the lower energy transfer. The fitted intercepts of the linear fits in Fig. 3, *a* and *b*, are ~0.27, and this corresponds to the measured value for the junctions singly labeled with the acceptor (0% donor). The square structure (Fig. 1) predicts the shortest donor-acceptor distance to be across right angles between neighboring arms for both vectors RH and XR of junction 3; the donor-acceptor distance for the vector XH would be larger, equal to the sum of two helical arm lengths across the square. Thus for the XH vector the energy transfer and, concomitantly, the slope would be less. This is what we observe and is the first physical measurement in solution that is at variance with the tetrahedral structure and consistent with the square global structure of the junction in the absence of higher salt concentrations. These data are in good agreement with the interpretation of experiments of the electrophoretic anomaly at low bivalent salt (Duckett et al., 1988) that the structure is square (see Fig. 5).

We can estimate the angles between the arms by assuming a simplified static molecular model for the DNA. The

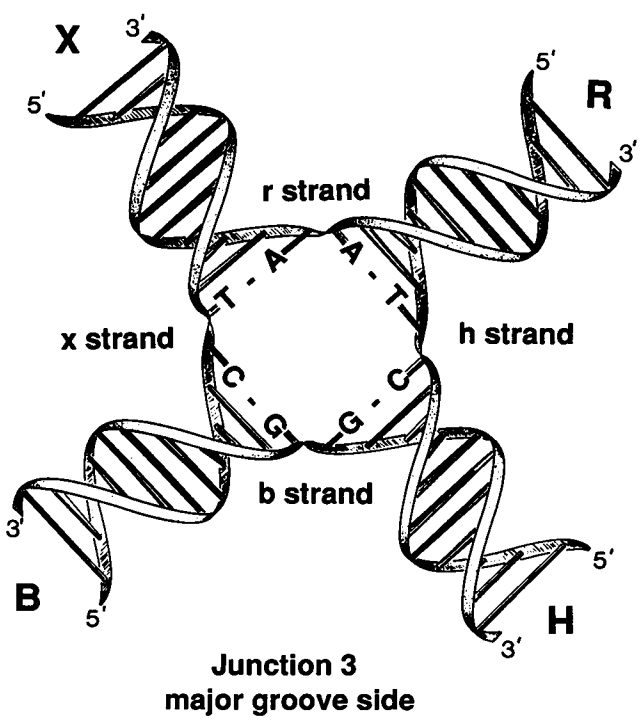

FIGURE 5 Ribbon model of the extended structure of the four-way DNA junction at low salt concentration. This illustrates the unstacked, extended structure in the absence of added cations, in which the four arms are extended toward the corners of a square. The junction has two inequivalent faces, where the central base pairs present either their major groove or their minor groove edges; the view shown is that of the major groove face. The inequivalence makes a pyramidal structure probable, and the apparent planarity of this illustration should not be assumed to be literal.

FRET efficiency has a maximum of ~5% in the low salt region (this maximum efficiency increases to ~15% in the folded form of the junction) (Murchie et al., 1989). We assume $\kappa^2 = 2/3$, which is a reasonable assumption in our case (Clegg et al., 1992). Using these E values and the relation $R = R_0[1/E - 1]^{1/6}$ we can calculate the angles between the arms (assumed to be rods) by simple trigonometry. For R_0 values ranging from 40 to 50 Å and for 17-basepair-length helical arms the acute angles estimated from the above efficiences are 55–71° for the high salt conditions and 69–90° for the low salt conditions. The angles between the arms at low salt conditions indicate that the square arrangement of the arms might not be planar (for a discussion of this, see below). In interpreting these values one must keep in mind the possible complications inherent in any FRET analysis (Clegg, 1992), the assumptions in using steady-state fluorescence to measure the efficiency of FRET (Clegg, 1992), and the oversimplified molecular model. In this regard we have shown previously (Clegg et al., 1992) that the steady-state measurements are consonant with time-resolved FRET measurements on the stacked X structure. The positions of the dye molecules relative to the DNA helices and the rotations of the helical arms about their axes relative to the other arms will modulate the *D-A* distances (Clegg et al., 1993). Time-resolved fluorescence experiments have been reported (Hochstrasser et al., 1992) with the purpose of estimating distributions in the positions of dye molecules covalently attached to DNA helices. The conformational distributions of flexible polymers can be extensive, and corresponding analyses have been implemented to investigate the distribution functions (Cantor and Pechukas, 1971; Haas et al., 1975) and kinetic aspects (Eisinger et al., 1969; Haas et al., 1978, Haas and Steinberg, 1984). The physical space available for dyes attached to double-stranded DNA molecules is limited by the rigidity of the helix. The distances between the dyes and the angles determined by us assuming a static dye-dye distance with a relatively small distribution are in a range consistent with both the square (low salt) and X (high salt) forms of the four-way junction with 17-bp arms.

Although both our electrophoretic and fluorescence experiments indicate a square arrangement of the helical arms at low salt concentrations, it is not required that the structure be planar, and pyramidal arrangements are equally consistent with the data. In fact, since the two sides of the junction are inequivalent (in the unfolded structure there is also a "major groove" side and a "minor groove" side, similar to the folded structure; see von Kitzing et al., 1990), it is quite probable that there will be some pyramidal distortion of planarity (see below).

An earlier study of a four-way junction of different sequence using transient electric birefringence (Cooper and Hagerman, 1989) reports a structure in the absence of Mg^{2+} that is different from the structure in the presence of Mg^{2+} and yet is also different from a square configuration of arms; their proposed structure is incompatible with their earlier electrophoretic results on the same junction molecules (Cooper and Hagerman, 1987). This may indicate that

electric birefringence is not well suited to the study of such complex polyelectrolyte structures (Diekmann and Pörschke, 1987), particularly since the extended structure in the absence of added ions may be distorted by high electric fields. We find complete agreement between our gel experiments and FRET results, with and without added Mg^{2+}. Without exception, all of the junction molecules that we have studied (this includes six fully paired junctions incapable of branch migration, two that may branch migrate by one step, and 18 junctions containing a single-base mismatch at the point of strand exchange) (Duckett and Lilley, 1991) give the same gel electrophoretic pattern indicative of the open structure in the absence of added ions; even though this is strong evidence that the structures are similar in all the cases investigated by us, we cannot exclude the possibility that there may be sequences with low salt conformations different from what we propose here.

Can we rationalize the approximate square structure at low salt?

The resistance of the four-way junction to folding into the stacked X structure at lower salt concentrations is likely due to strong electrostatic repulsion forces that must be compensated for in order to stabilize the folded structure. One of the major stabilizing factors of the stacked X structure is probably the favorable free energy of base pair stacking between the base pairs flanking the neighboring helical arms (Duckett et al., 1988; Murchie et al., 1989; Clegg et al., 1992). Apparently strong electrostatic repulsions between closely spaced phosphate charges (possibly at the exchange point) must be screened before this stacked conformation can form. Upon stacking, a close interaction of the two quasi-continuous helices is then possible provided that the right-handed X structure is formed. If the helices are oriented this way, one of the phosphate strands of one helix can fit over the major groove of the other helix, thereby minimizing the unfavorable van der Waals and electrostatic interactions (von Kitzing et al., 1990). Mg^{2+} is probably the natural counterion needed to achieve the necessary ion screening, but we have shown that Ca^{2+} is almost as effective and that Na^{+} alone also allows the junction to fold globally at higher ion concentrations (Clegg et al., 1992).

However, at low salt the screening action of the surrounding ions is insufficient to override the unfavorable electrostatic repulsions between the phosphates. The junction must then adjust to a more extended conformation in order to minimize the overall free energy; strong electrostatic interactions and van der Waals restrictions probably impose constraints upon the molecular orientations of the helical arms.

Is it reasonable, from the point of view of only electrostatic repulsions, to assume that the low salt structure is approximately a square? The helical arms are connected by the continuous intertwined single strands. At least one phosphate is positioned between each pair of helical arms (defined by Fig. 1 *a*). If we assume that there are no preferential interactions between any pair of neighboring arms (such as that found in the stacked X structure) then the structure probably would have symmetrically disposed arms. Assume, for the moment, that this is the case. The simplest model of the phosphate distribution about the center point of the junction consists of four phosphate charges connected to each other across the faces of the center flanking base pairs. If we consider only the electrostatic repulsion forces between these four phosphates to be active in such a simple restricted system, what would be the three-dimensional charge distribution with the minimum energy? The charges would tend to separate maximally from each other, and this would lead to a square arrangement. However, we would not necessarily expect a perfect planar structure; and indeed, it has been realized previously that a minor and major groove face of such a square extended junction structure is expected (von Kitzing et al., 1990). On the other hand, were the charges free to move on the surface of a sphere, in a spherically symmetric fashion about the center point (e.g., if they were charged rods connected at the ends at the center point), the electrostatic forces would tend to arrange the arms in a tetrahedral fashion (with equivalent FRET signals), and this does not agree with our experimental results. This is not to say that the actual electrostatic forces can necessarily be modeled according to such simple ideas; and surely there are other important, and perhaps overriding, physical considerations. However, considering the problem from this point of view it is perhaps not surprising that our results are consistent with a square structure at low salt concentrations.

Fluorescence anisotropy measurement of FRET

The extent of energy transfer between two labeled arms of the junction 3 molecule at higher salt concentrations previously measured by other methods (Clegg et al., 1992) is seen to account for the FRET acceptor anisotropy measurements shown in Fig. 4. Usually the fluorescence anisotropy of the donor is used to detect energy transfer (Weber, 1960a,b). However, as discussed above, provided that the acceptor has sufficient anisotropy, it is possible to measure FRET by observing the fluorescence anisotropy of the acceptor. The agreement between the $r_{490,\ 590}$ measurements of the donor titrations and the expected values based on our earlier published measurements (Clegg et al., 1992), lends further support for the stacked X structure of the four-way junction at higher salt conditions. In addition, the assumption that the anisotropy of the donor is sufficiently low to approximate the angular factor κ^2 to be $\sim 2/3$ is further justified. We have used this analysis method subsequently to estimate E values from FRET for a series of bulge molecules, and good agreement between the estimates for E from the anisotropy measurements and the more conventional analyses was found (C. Gohlke et al., manuscript in preparation).

Possible biological relevance of the extended low salt structure

Since the ionic concentration inside cells is greater than the level required to fold the four-way junction, the extended

structure is unlikely to exist stably in vivo, at least in the absence of proteins. However, this structure may resemble a transient intermediate in dynamic processes such as isomerization and branch migration. Moreover, this study emphasizes the important role played by cations in the folding of the junction, inducing a major conformational change.

In this work we have used a number of new FRET approaches, including the global comparison of vectors, the titration of donor labeling, and the use of anisotropies, to obtain useful information on the geometry and transitions in an important DNA structure. We expect that FRET will be more widely used in investigations of nucleic acid structures, just as this well-established technique has been usefully applied to numerous biological and polymeric systems (Stryer, 1978; Valeur, 1989).

We thank Dr. S. Diekmann for discussion, Dr. E. v. Kitzing for collaboration on theoretical aspects of the four-way junction structure, and Annelies Zechel for excellent technical assistance.

We are indebted to NATO for a travel grant and the SERC, MRC, and CRC for financial support.

REFERENCES

Beaucage, S. L., and M. H. Caruthers. 1981. Deoxynucleoside phosphoramidites—a new class of key intermediates for deoxypolynucleotide synthesis. *Tetrahedron Lett.* 22:1859–1862.

Bennett, R. G. 1964. Radiationless intermolecular energy transfer. I. Singlet→triplet transfer. *J. Chem. Phys.* 41:3037–3040.

Cantor, C. R., and P. Pechukas. 1971. Determination of distance distribution functions by singlet-singlet energy transfer. *Proc. Natl. Acad. Sci. USA.* 68:2099–2101.

Cardullo, R. A., S. Agrawal, C. Flores, P. C. Zamecnik, and D. E. Wolf. 1988. Detection of nucleic acid hybridization by nonradiative fluorescence resonance energy transfer. *Proc. Natl. Acad. Sci. USA.* 85:8790–8794.

Churchill, M. E., T. D. Tullius, N. R. Kallenbach, and N. C. Seeman. 1988. A Holliday recombination intermediate is twofold symmetric. *Proc. Natl. Acad. Sci. USA.* 85:4653–4656.

Clegg, R. M. 1992. Fluorescence resonance energy transfer and nucleic acids. *In* Methods in Enzymology. D. M. J. Lilley and J. E. Dahlberg, editors. Academic Press, San Diego. 353–388.

Clegg, R. M., A. I. H. Murchie, A. Zechel, C. Carlberg, S. Diekmann, and D. M. J. Lilley. 1992. Fluorescence resonance energy transfer analysis of the structure of the four-way junction. *Biochemistry.* 31:4846–4856.

Clegg, R. M., A. I. H. Murchie, A. Zechel, and D. M. J. Lilley. 1993. Observing the helical geometry of double-stranded DNA in solution by fluorescence resonance energy transfer. *Proc. Natl. Acad. Sci. USA.* 90: 2994–2998.

Connolly, B. A. 1987. The synthesis of oligonucleotides containing a primary amino group at the 5′ terminus. *Nucleic Acids Res.* 15:3131–3139.

Conrad, R. H., and L. Brand. 1968. Intramolecular transfer of excitation from tryptophan to 1-dimethylaminonaphtalene-5-sulfonamide in a series of model compounds. *Biochemistry.* 7:777–787.

Cooper, J. P., and P. J. Hagerman. 1987. Gel electrophoretic analysis of the geometry of a DNA four-way junction. *J. Mol. Biol.* 198:711–719.

Cooper, J. P., and P. J. Hagerman. 1989. Geometry of a branched DNA structure in solution. *Proc. Natl. Acad. Sci. USA.* 85:4653–4656.

Dale, R. E., J. Novrus, S. Roth, M. Edidine, and L. Brand. 1981. Application of Förster long-range excitation energy transfer to the determination of distributions of fluorescently-labelled concanavalin A-receptor complexes at the surfaces of yeast and of normal and malignant fibroblasts. *In* Fluorescent Probes. G. S. Beddard and M. A. West, editors. Academic Press, London. 159–181.

De Boeck, H., R. B. J. MacGregor, R. M. Clegg, N. Sharon, and F. G. Loontiens. 1985. Binding of *N*-dansylgalactosamine to the lectin from *Erythrina cristagalli* as followed by stopped-flow and pressure-jump relaxation kinetics. *Eur. J. Biochem.* 149:141–148.

Dewey, T. G. 1992. Fluorescence resonance energy transfer on fractals. *Acc. Chem. Res.* 25:195–200.

Diekmann, S., and D. Pörschke. 1987. Electro-optical analysis of curved DNA fragments. *Biophys. Chem.* 26:207–216.

Drake, J. M., J. Klafter, and P. Levitz. 1991. Chemical and biological microstructures as probed by dynamic processes. *Science (Washington DC).* 251:1574–1579.

Duckett, D. R., and D. M. J. Lilley. 1991. Effects of base mismatches on the structure of the four-way DNA junction. *J. Mol. Biol.* 221:147–161.

Duckett, D. R., A. I. H. Murchie, S. Diekmann, E. von Kitzing, B. Kemper, and D. M. J. Lilley. 1988. The structure of the Holliday junction and its resolution. *Cell.* 55:79–89.

Duckett, D. R., A. I. H. Murchie, and D. M. J. Lilley. 1990. The role of metal ions in the conformation of the four-way junction. *EMBO J.* 9:583–590.

Eisinger, J., B. Feuer, and A. A. Lamola. 1969. Intramolecular singlet excitation transfer. Application to polypeptides. *Biochemistry.* 8:3908–3915.

Förster, T. 1948. Zwischenmolekulare Energiewanderung und Fluoreszenz. *Ann. Phys.* 2:55–75.

Förster, T. 1949. Experimentelle und theoretische Untersuchung des zwischenmolekularen Übergangs von Elektronenregungsenergie. *Z. Naturforsch.* 5:321–327.

Förster, T. 1951. Fluoreszenz Organischer Verbindungen. Vandenhoeck and Ruprecht, Göttingen, Germany.

Gough, G. W., and D. M. J. Lilley. 1985. DNA bending induced by cruciform formation. *Nature (Lond.).* 313:154–156.

Haas, E., and I. Z. Steinberg. 1984. Intramolecular dynamics of chain molecules monitored by fluctuations in efficiency of excitation energy transfer. *Biophys. J.* 46:429–437.

Haas, E. H., E. Wilchek, E. Katchalski-Katzir, and I. Z. Steinberg. 1975. Distribution of end-to-end distances of oligopeptides in solution as estimated by energy transfer. *Proc. Natl. Acad. Sci. USA.* 72: 1807–1811.

Haas, E., E. Katchalski-Katzir, and I. Z. Steinberg. 1978. Brownian motion of the ends of oligopeptide chains in solution as estimated by energy transfer between the chain ends. *Biopolymers.* 17:11–31.

Hauser, M., U. K. A. Klein, and U. Gösele. 1976. Extension of Förster's theory of long-range energy transfer to donor-acceptor pairs in systems of molecular dimensions. *Zeitschr. Phys. Chem. Neue Folge.* 101: 255–266.

Hochstrasser, R. A., S-M. Chen, and Millar, D. P. 1992. Distance distribution in a dye-linked oligonucleotide determined by time-resolved fluorescence energy transfer. *Biophys. Chem.* 45:133–141.

Hoess, R., A. Wierzbicki, and K. Abremski. 1987. Isolation and characterization of intermediates in site-specific recombination. *Proc. Natl. Acad. Sci. USA.* 84:6840–6844.

Holliday, R. 1964. A mechanism for gene conversion in fungi. *Genet. Res.* 5:282–304.

Jayaram, M., K. L. Crain, R. L. Parsons, and R. M. Harshey. 1988. Holliday junctions in FLP recombination: resolution by step-arrest mutants of FLP protein. *Proc. Natl. Acad. Sci. USA.* 85:7902–7906.

Jovin, T. M. 1991. Parallel-stranded DNA with *trans*-Crick-Watson base pairs. *In* Nucleic Acids and Molecular Biology. F. Eckstein and D. M. J. Lilley, editors. Springer-Verlag, Heidelberg. 25–38.

Jovin, T. M., and D. J. Arndt-Jovin. 1989. FRET microscopy: digital imaging of fluorescence resonance energy transfer. Application in cell biology. *In* Cell Structure and Function by Microspectrofluorometry. E. Kohen, Ploem, J. S., and J. G. Hirshberg, editors. Academic Press, Inc., Orlando. 99–117.

Kitts, P. A., and H. A. Nash. 1987. Homology-dependent interactions in phage λ site-specific recombination. *Nature (Lond.).* 329:346–348.

Kubitscheck, U., M. Kircheis, R. Schweitzer-Stenner, W. Dreybrodt, T. M. Jovin, and I. Pecht. 1991. Fluorescence energy transfer on living cells. Application to binding of monovalent haptens to cell-bound immunoglobulin E. *Biophys. J.* 60:307–318.

Mataga, N., H. Obashi, and T. Okada. 1969. Electronic excitation transfer from pyrene to perylene by a very weak interaction mechanism. *J. Phys. Chem.* 73:370–374.

McClellan, J. A., and D. M. J. Lilley. 1987. A two-state conformational equilibrium for alternating (A-T)n sequences in negatively supercoiled DNA. *J. Mol. Biol.* 197:707–721.

Meselson, M. S., and C. M. Radding. 1975. A general model for genetic recombination. *Proc. Natl. Acad. Sci. USA.* 72:358–361.

Murchie, A. I. H., R. M. Clegg, E. von Kitzing, D. R. Duckett, S. Diekmann, and D. M. J. Lilley. 1989. Fluorescence energy transfer shows that the four-way DNA junction is a right-handed cross of antiparallel molecules. *Nature (Lond.).* 341:763–766.

Nunes-Düby, S. E., L. Matsomoto, and A. Landy. 1987. Site-specific recombination intermediates trapped with suicide substrates. *Cell.* 50:779–788.

Orr-Weaver, T. L., J. W. Szostak, and R. J. Rothstein. 1981. Yeast transformation: a model system for the study of recombination. *Proc. Natl. Acad. Sci. USA.* 78:6354–6358.

Perrin, J. 1927. Fluorescence et induction moléculare par resonance. *Compt. Rend. Acad. Sci.* 184:1097–1100.

Rippe, K., V. Dötsch, and T. M. Jovin. 1993. Confirmation of strand orientation in parallel-stranded and anti-parallel-stranded DNA duplexes by fluorescence resonance energy transfer and pyrene eximer fluorescence. *In* DNA, Interaction with Ligands and Proteins. Problems of Recognition and Self-Organization. Fundamental Aspects and Technical Trends. E. A. T. Funck, editor. Nova Science Publishers, St. Petersburg, Russia.

Sinha, N. D., J. Biernat, J. McManus, and H. Koster. 1984. Polymer support oligonucleotide synthesis XVIII: use of β-cyanoethyl-*N,N*-dialkylamino/*N*-morpholino phosphoramidite of deoxynucleosides for the synthesis of DNA fragments simplifying deprotection and isolation of the final product. *Nucleic Acids Res.* 12:4539–4557.

Steinberg, I. Z. 1968. Nonradiative energy transfer in systems in which rotary brownian motion is frozen. *J. Chem. Phys.* 48:2411–2413.

Stryer, L. 1978. Fluorescence energy transfer as a spectroscopic ruler. *Annu. Rev. Biochem.* 47:819–846.

Szöllósi, J., L. Trón, S. Damjanovich, S. H. Helliwell, D. Arndt-Jovin, and T. M. Jovin. 1984. Fluorescence energy transfer measurements on cell surfaces: a critical comparison of steady-state fluorimetric and flow cytometric methods. *Cytometry.* 5:210–216.

Valeur, B. 1989. *In* Fluorescent Biomolecules: Methodologies and Applications. D. M. Jameson and G. D. Reinhart, editors. Plenum Press, New York. 269–303.

von Kitzing, E., D. M. J. Lilley, and S. Diekmann. 1990. The stereochemistry of a four-way DNA junction: a theoretical study. *Nucleic Acids Res.* 18:2671–2683.

Weber, G. 1960a. Fluorescence-polarization spectrum and electronic-energy transfer in tyrosine, tryptophane and related compounds. *Biochem. J.* 75:335–345.

Weber, G. 1960b. Fluorescence-polarization spectrum and electronic-energy transfer in proteins. *Biochem. J.* 75:345.